

Organic transistors fabricated by contact coating at liquid-solid interface for nano-structures

Yu-Wen Cheng, Chao-Hsuan Chen, Hsin-Fei Meng^{*}, Hsiao-Wen Zan^{*}, Yu-Chiang Chao^{*}, and Sheng-Fu Horng

Citation: *AIP Advances* **5**, 107146 (2015); doi: 10.1063/1.4935188

View online: <http://dx.doi.org/10.1063/1.4935188>

View Table of Contents: <http://aip.scitation.org/toc/adv/5/10>

Published by the [American Institute of Physics](#)

Organic transistors fabricated by contact coating at liquid-solid interface for nano-structures

Yu-Wen Cheng,¹ Chao-Hsuan Chen,² Hsin-Fei Meng,^{1,a} Hsiao-Wen Zan,^{2,b}
Yu-Chiang Chao,^{3,c} and Sheng-Fu Horng⁴

¹*Institute of Physics, National Chiao Tung University,
Hsinchu 300, Taiwan, Republic of China*

²*Department of Photonics and the Institute of Electro-Optical Engineering,
National Chiao Tung University, Hsinchu 300, Taiwan, Republic of China*

³*Department of Physics, Chung Yuan Christian University,
Taoyuan 320, Taiwan, Republic of China*

⁴*Department of Electrical Engineering, National Tsing Hua University,
Hsinchu 300, Taiwan, Republic of China*

(Received 11 August 2015; accepted 20 October 2015; published online 30 October 2015)

A contact coating method is developed to cover the nano-channels with 100 nm or 200 nm diameter and 400 nm depth with a poly(4-vinylphenol) (PVP). In such coating the nano-channels faces downwards and its vertical position is controlled by a motor. The surface is first lowered to be in immediate contact with the polyvinylpyrrolidone (PVPY) water solution with concentration from 1 to 5 wt%, then pulled at the speed of 0.004 to 0.4 mm/s. By tuning the pulling speed and concentration we can realize conformal, filled, top-only, as well as floating film morphology. For a reproducible liquid detachment from the solid, the sample has a small tilt angle of 3 degree. Contact coating is used to cover the Al grid base of the vertical space-charge-limited transistor with PVPY. Poly(3-hexylthiophene-2,5-diyl) (P3HT) as the semiconductor. The transistor breakdown voltage is raised due to base coverage achieved by contact coating. © 2015 Author(s). All article content, except where otherwise noted, is licensed under a Creative Commons Attribution 3.0 Unported License. [<http://dx.doi.org/10.1063/1.4935188>]

I. INTRODUCTION

Thin film coating by solution is a relatively mature technology for planar solid surface. Uniform film with nanometer precision can be made by spin coating, slot die coating, or blade coating.¹ For a given material, the only parameter for the coated film on planar surface is its thickness. The general method of solution coating on surface with nano-structures is far more unknown. Unlike the case of planar surface coating, there are many conceivable ways for the film to cover the solid nano-structures. For example it could fully fill in the valley of the structures or float over the peaks and leaves some voids beneath. From the application point of view, there are many device structures requiring a hetero-junction on nano-structured rather than planar surface. In solid-state dye-sensitive solar cell the hole-transport organic material is deposited on top of the inorganic electron-transport nano-porous structures of oxide semiconductors like ZnO or TiO₂.² In silicon hybrid solar cells the p-type conducting polymer is deposited over silicon nano-wires³ to form p-n junction. For chemical sensors the organic chemical probe materials are often coated over the inorganic nano-wires.⁴ For both the solar cell and sensor the nano-structure has the advantage of large contact area compared with planar surfaces. Furthermore, in the case of vertical-type transistors the insulators may need to cover the vertical gate as the gate dielectric in case of field-effect transistor.⁵

^aElectronic mail: meng@mail.nctu.edu.tw

^bElectronic mail: hsiaowen@mail.nctu.edu.tw

^cElectronic mail: ychao@cycu.edu.tw

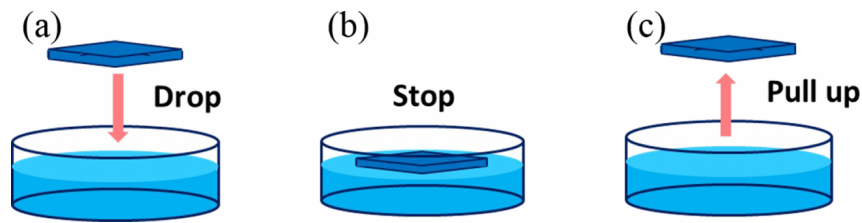


FIG. 1. (a)-(c) The schematic diagram of contact coating process.

One kind of vertical transistor is vacuum-tube like, and is sometimes called solid-state triode or permeable base transistor. For such vacuum-tube like vertical transistors the insulator may need to cover the metal base with nano-grid structure.⁶ Among all the possible ways of thin film coverage, conformal coating attracts a particularly high interest. For vacuum process atomic-layer-deposition (ALD) is a well-known method to achieve conformal coverage of arbitrary structures. For solution process the conventional coating methods do not give a well-controlled conformal coverage. Spin coating of conjugated polymer is reported to give floated film over the peaks of the silicon nano-wires,⁷ while spin coating of small molecule fills inside the nano-wires.⁸ Dip-coating is well-known to cover the surface of nano-wires with self-assembled mono-layers (SAM) but the thickness is limited to less than a few nano-meters.⁹ Immersion of nano-wires in the solution leads core-sheath structure after drying.¹⁰ Coating by the contact of the substrate and the liquid surface is also studied.^{11,12} So far there is no report on a coating platform by which the morphology and thickness of the covering film can be finely tuned on nano-structures.

In this paper we report a contact coating method where the sample with nano-structured surface is kept downward and in contact with the liquid surface of the solution as shown in Fig. 1. The sample substrate is not immersed in the solution but suspended at the position of immediate liquid-solid contact. After reaching equilibrium the sample is pulled up with a controlled speed as shown in Fig. 2 and 3. How the solution penetrates inside the nano-structures will be determined by the interplay of solution surface tension, contact angle with the solid surface, as well as the pulling speed. It turns out that a wide range of coating morphology and thickness can be reproducibly made by tuning the pulling speed and the concentration of the solution. For low concentration and low viscosity we may obtain conformal or filled coverage of nano-holes with 100-200 nm diameters. For higher concentration and viscosity we may obtain floating or top-only coverage. This contact coating is used to cover the metallic grid base of vertical type space-charge-limited transistors (SCLT), shown in Fig. 4, by an insulating polymer polyvinylpyrrolidone (PVPY). Without such insulator the aluminum base is in direct contact with the organic semiconductor poly(3-hexylthiophene-2,5-diyl) (P3HT), and the transistor may have large base leakage current at high operation voltage. After base coverage of PVPY both the leakage current to the collector and from the emitter electrodes are significantly reduced. This is, however, only the first example of contact coating method to form a covering film without filling the nano-structures. With such controlled coating over a wide range of coverage morphology, contact coating may be useful in other areas like hybrid solar cell or chemical sensors.

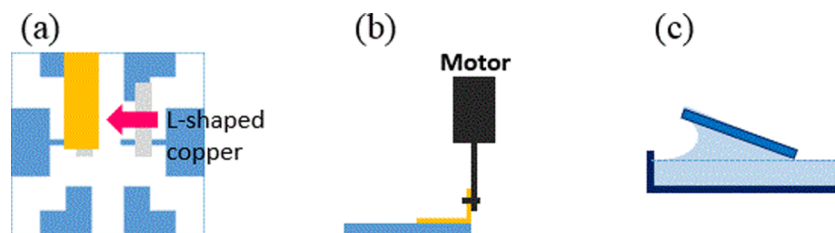


FIG. 2. (a) The position of L-shaped copper, (b) The schematic diagram of contact coating system, and (c) Sample tilts a small angle from horizontal.

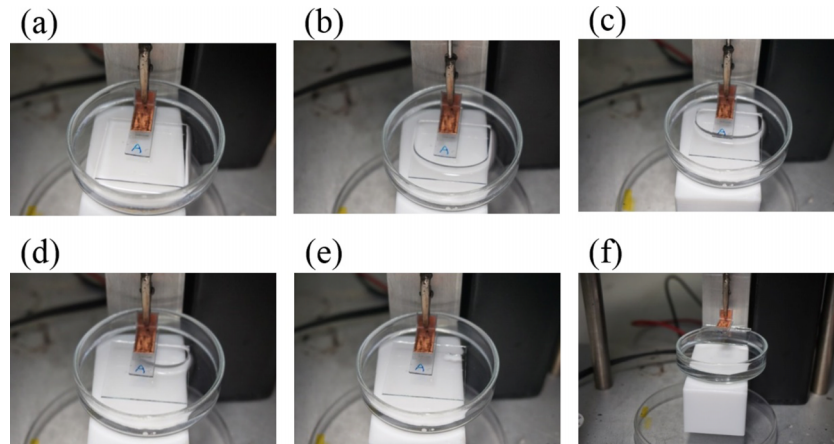


FIG. 3. (a)-(f) The pictures of contact coating process.

II. CONTACT COATING SETUP

The process of contact coating is schematically shown in Fig. 1. The face of the samples with nano-structures are kept downward by fixing it on the horizontal arm of a L-shaped copper as shown in Fig. 2(a). The other arm of the copper is kept vertical and is connected to a motor which is not shown in the figure. The motor can lower or raise the vertical position of the sample with controlled speed. The material to be coated is dissolved in solution inside a container. The sample is lowered and stopped right after the downward surface is in contact with the liquid surface as shown in Fig. 1(a). After a few seconds of contact time for the solution to be in equilibrium with the solid surface, the sample is pulled up with fixed speed as shown in Fig. 1(c). Note that the sample is not immersed in the solution but suspended at the position of first contact with the liquid surface. During the pulling up time the liquid surface gradually detach from the solid surface as shown in the pictures of Fig. 3. In order to achieve a uniform and reproducible results the sample is tilted from horizontal by a small angle around 3 degree as shown in Fig. 2(c). Assuming that the left of the sample is slightly higher than the right, during liquid detachment the left part will be exposed to air earlier than the right part, and there will be a moving boundary of the exposed part. In other words, this boundary is between the sample surface part that already left and solution and the part

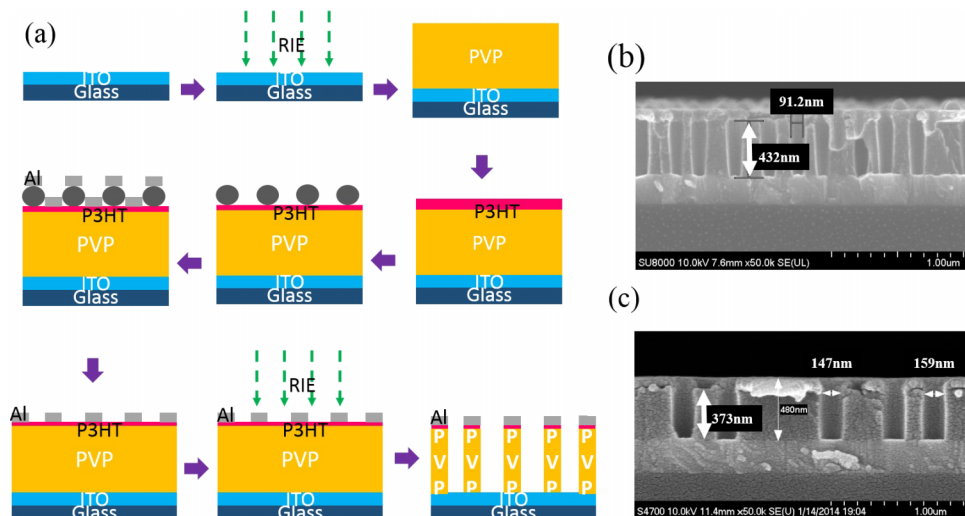


FIG. 4. (a) The schematically of the nano-channel structure fabrication process. Cross-section SEM image of the device structure fabricated with (b) 100 nm and (c) 200 nm.

that is still in contact with the solution. During the pulling period the boundary will sweep across the entire sample surface and eventually disappear as the sample completely leaves the solution. The evolution of the liquid boundary is shown in the pictures of Fig. 3. In (a) the entire sample is in contact with the solution and there is no boundary. In (b)-(c) the boundary moves from the bottom to the top in the pictures. In reality it moves horizontally toward the L-shaped copper which holds the sample and keeps it at a small tilted angle. In (e) the sample just left the liquid surface, whereas in (f) the sample is high above the liquid surface. In case that the solution is not dry after pulling, the sample is kept in position (f) for drying. Without such small artificial tilt angle the liquid boundary may sweep across the sample surface in an unpredictable way and the some variation in coating results may occur. The range of the pulling speed is 0.04 mm/second to 0.4 mm/second in this work. For a given material and solvent, the solution concentration and the pulling speed are the two critical parameters for contact coating method. For low pulling speed like 0.004 mm/s the detachment period in (a)-(f) may takes over 15 minutes. The drying in position (f) is usually 15 minutes. In general the total amount of solution left on the surface increases significantly with the increasing pulling speed. For slow speed the solution seems to be pulled back to the container by the viscosity in the final phase of detachment. For higher speed there is not enough time for the liquid to be pulled back.

III. FABRICATION OF NANO-CHANNELS

In this work the nano-structure is fabricated by the colloid lithography using random distribution of polystyrene (PS) spheres with diameters 100 nm or 200 nm. The spheres are used as the shadow mask for metal evaporation. After removal of the spheres by tape the nano-channels are created by vertical reactive ion etching (RIE) through opening of the metal. The process is schematically shown in Fig. 4(a) and described in details below. The patterned ITO substrate was first immersed into acetone and isopropyl alcohol respectively with ultrasonic agitation for 5 minutes. Then, we rinsed the substrates by DI water, dried by N₂ gas flow, and put on the hot plate to remove residue water. Afterwards, substrates are sent to RIE system to treat the ITO surface by oxygen plasma for 10 minutes. We spin-coated a 400nm Poly(4-vinylphenol) (PVP), and annealed at 200° C for 1 hour. The surface of PVP was spin -coated by a poly(3-hexylthiophene-2,5-diyl) (P3HT) (1.5 wt% at chlorobenzene) film and annealed at 200° C for 10 minutes again. We then used xylene to spin-rinse superfluous P3HT. The substrates were merged into a 0.2wt% PS sphere solution of ethanol. The diameter of PS spheres are 100 and 200 nm. After immersing for 90 seconds, the substrate was taken out of the solution and rinsed by ethanol immediately. Then, we put the substrate into boiling isopropyl alcohol for 10 second to remove residue polystyrene spheres. Then we dried to the sample by N₂ gas flow as soon as we took it out from isopropyl alcohol. After these steps, PS spheres were attached on the surface and form a non-close-packed matrix.

These polystyrene spheres can serve as shadow mask. A 40-nm aluminum was deposited on the surface. After removing the polystyrene spheres by an adhesive tape (Scotch, 3M), the PVP at sites without Al coverage is removed by 900 second, 70 W O₂ plasma RIE. Finally we obtain a metal-grid-structure substrate. The scanning electron microscope (SEM) images of the finished nano-channels are shown in Fig. 4(b), 4(c).

IV. MORPHOLOGY AFTER COATING

In this work we coat the cross-linking polymer polyvinylpyrrolidone (PVPY) dissolved in DI water over the nano-channels using contact coating method. PVPY cross-links under ultraviolet (UV) illumination. It is purchased from Sigma Aldrich. Note that this PVPY is chemically different from the PVP used in the nano-channels above. Their chemical structures are shown in Fig. 5(a) and Fig. 5(b) respectively. After coating the sample is illuminated by UV with 257.9 nm wavelength for 2 hours at the irradiance 30 mW/cm² for cross-linking. The UV step is to enhance the insulating property required for the vertical transistor application to be discussed below. For film morphology the UV illumination is not important. As discussed above the two most important parameters for

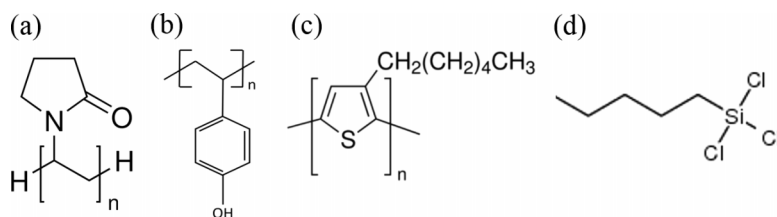


FIG. 5. Chemical structures of the materials. (a) Polyvinylpyrrolidone (PVPY), (b) Poly(4-vinylphenol) (PVP), (c) Poly(3-hexylthiophene) (P3HT), and (d) Octadecyltrichlorosilane (OTS-18).

contact coating is the pulling speed and the solution concentration. Higher concentration gives higher solution viscosity.

Before discussing the SEM images we show four types of coating results A, B, C, and D in Fig. 6. Between the two PVP sidewalls there is the cylindrical nano-channels. Note that in our sample we have nano-channels rather than nano-rods, these two cases are not differentiated in the schematic cross section picture. In type A the PVPY, marked in green, has a conformal coverage of the entire nano-channels including its top, sidewall, and bottom. It is called “conformal type” below. In type B the PVPY not only penetrate inside the nano-channel but also fills in completely, so the channel no longer exists. It is called “filled type” below. In type C the PVPY does not penetrate deeply inside the nano-channel but stay outside. It covers only the top portion of the nano-structures, and is called “top-only type” below. In type D the PVPY on the top merges into a single film floating on top of the nano-channels and left a cavity beneath. It is called “floating type” below. In Fig. 6 we also give a speculation on the state of the liquid-solid interface when they are

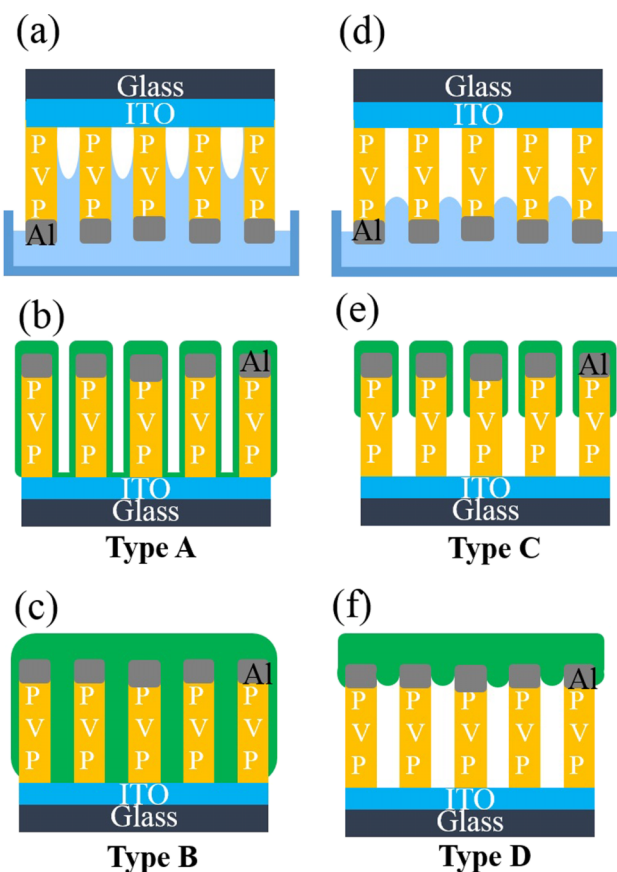


FIG. 6. (a)-(f) Four types of coating results.

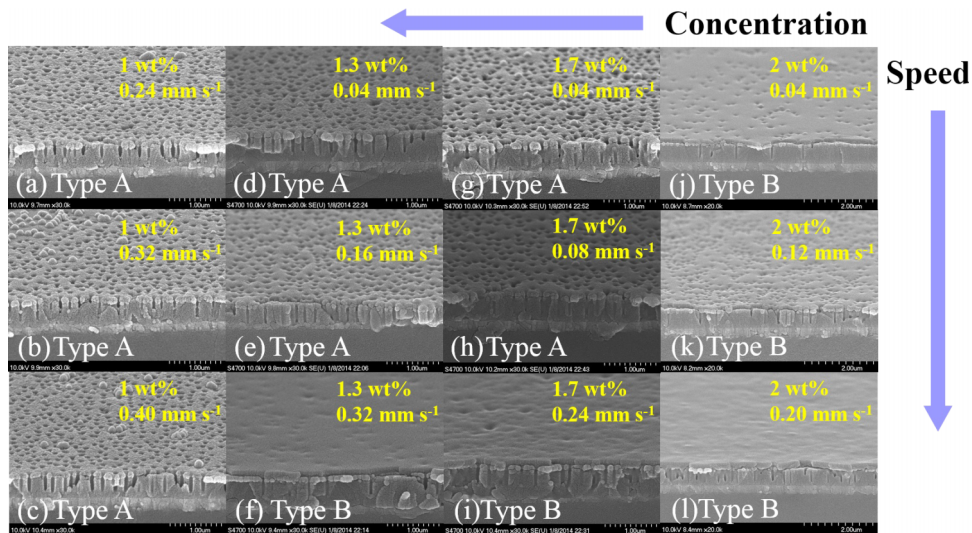


FIG. 7. (a)-(l) Side-view SEM images of the nano-channel with 400 nm depth and 100 nm diameter.

in contact, i.e. permeating inside the nano-structure in Fig. 6(a) and stopped at the tips in Fig. 6(d). For types A and B there is a tendency for the solution to penetrate inside the nano-channel, so the solution may move up into the channel by the capillary action as shown in Fig. 6(a). There is probably a low local contact angle. The major difference between A and B is that there is more material left on the substrate in B so the channel side walls merge. On the other hand for types C and D there is a tendency for the solution to stay outside of the nano-channels. The speculated state in the liquid-solid contact is shown in Fig. 6(d). There is probably a large local contact angle and the deep part of the channels is not wetted. Type D has more material than type C such that the coated material on the top merges to form a single film. The SEM images for the nano-channel with 400 nm depth and 100 nm diameter are shown in Fig. 7 for various pulling speed and PVPY concentration in DI water. As the speed increases in general there is a change from the conformal type A to a filled type B. The reason is that the total amount of solution left on the surface increases significantly with the increasing pulling speed. More solution means more PVPY and higher chance for the sidewalls to merge. As we increase the solution concentration we obtain thicker film on the top in general. For low concentration like 1 wt% the PVPY is so thin that the granular structure of the Al surface is still visible, whereas for high concentration over 1.3 wt% the top surface is rather smooth implying a thick polymer on top. The thickness can be roughly estimated by the SEM cross section images. For example it is 30 nm in Fig. 7(a) and 55 nm in Fig. 7(e). The details of the coating at 2 wt% and 0.04 mm/s pulling speed is shown in Fig. 8(a) to demonstrate the conformal coating. For comparison, the original 100 nm channels before contact coating are shown in Fig. 4(b). The most conspicuous feature of the coated sample is that the original 100 nm channel is shrunk into a narrow channel with diameter around 50 nm. PVPY is seen in both the top, the

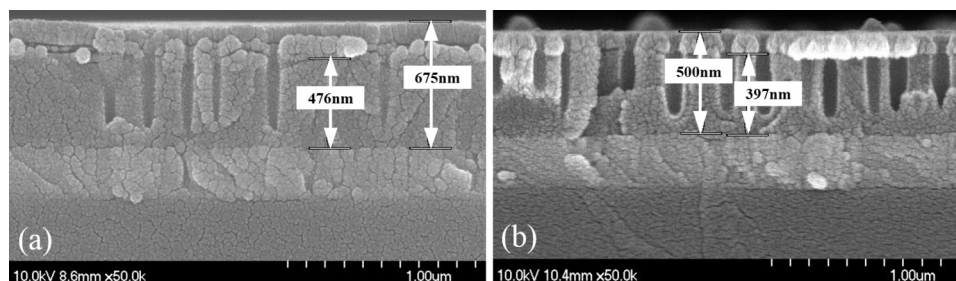


FIG. 8. Cross-section SEM images of the nano-channel coated with (a) 2 wt% and 0.04 mm s^{-1} and (b) 1 wt% and 0.4 mm s^{-1} .

sidewall and the bottom of the channels. Such conformal coating is only realized before in the atomic layer deposition through gas-phase precursors. Here it is simply achieved with a polymer dissolved in water. The thickness of PVPY is estimated to be 60 nm on top, 25 nm on the sidewall, and 90 nm on the bottom. Another example is shown in detail in Fig. 8(b) for 1 wt% and 0.4 mm/s pulling speed. The interface between the PVPY and the PVP happens to be visible. The thickness of PVPY is estimated to be 40 nm on top, 5 nm on the sidewall, and 100 nm on the bottom.

The SEM images of the nano-channels with 200 nm diameter are shown in Fig. 9 for various pulling speed and concentration. Similar to the case of 100 nm channel, there is a trend to change from the conformal type A to filled type B as the pulling speed increases. Here we study some high concentrations which is not used for 100 nm channel. For 4 wt% we obtain the top-only type C. As shown in Fig. 9(g) for 0.004 mm/s the thick PVPY on top of Al is apparent but the bottom of the nano-channel remains flat, indicating that the PVPY does not penetrate deeply inside the channel. It is therefore not the conformal type A. As the pulling speed increases to 0.04 mm/s the PVPY on the top merges into a thick uniform film and the dip of the nano-channels is no longer visible from the top. The cross section images show that the PVPY does not fill up the channels but leave a cavity beneath. Similar results are obtained for 5 wt%. Higher concentration of PVPY gives much higher viscosity and consequently surface tension. The high surface tension may prevent the solution from penetrating inside the nano-channels as shown in Fig. 6(d). We therefore obtain the floating type D for high concentration and high pulling speed. Apparently the types of the coating results is expected to depend on the surface energy of the channel sidewall. To confirm this we compare same coating condition for the channel with self-assembled monolayer (SAM) treatment and without. SAM of octadecyltrichlorosilane (OTS-18) is deposited on nano-channel by immersion for 2 hours. For pulling speed at 0.12 mm/s and concentration of 3 wt%, the filled type C would result without SAM. For SAM of OTS the floating type D results as shown in Fig. 10. There is a thick PVPY to seal the channel but the sidewall remains clean. It is well-known that OTS surface treatment converts a hydrophilic surface with many OH groups into a hydrophobic surface with alkyl terminals. Such hydrophobic surface repels the water solution and keep the PVPY outside of the nano-channels. Finally for comparison we show the results for two other coating methods, the dip coating and spin coating. In the former the sample is vertically immersed into the solution and pulled up. The result is shown in Fig. 11 with 3 wt% and 0.004 mm/s. It turns out that dip coating does not give a consistent coating morphology as shown in Fig. 11(b). For the three consecutive channels there are conformal type, top-only type and floating type. For spin coating the PVPY appears only at the bottom of the channel as shown in Fig. 11(c).

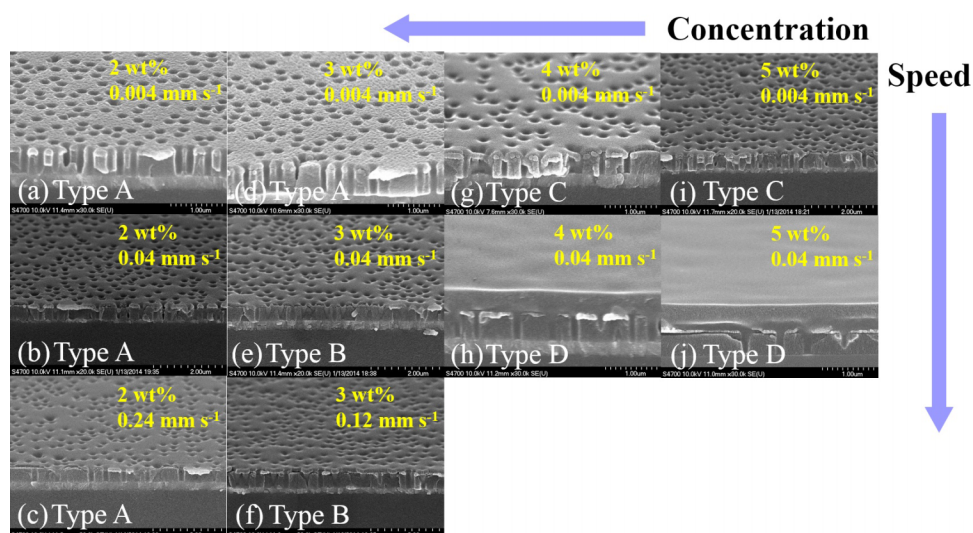


FIG. 9. (a)-(j) Side-view SEM images of the nano-channel with 400 nm depth and 200 nm diameter.

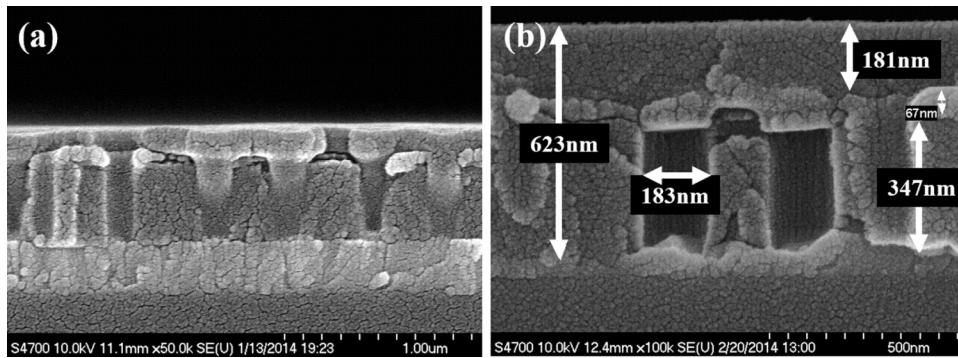


FIG. 10. Cross-section SEM images of the nano-channel coated (a) without SAM and (b) with SAM.

V. VERTICAL TRANSISTOR

We apply the contact coating method above to improve the performance of the vertical space-charge-limited transistor (SCLT) as the first device example. SCLT is a solid-state version of vacuum tube triode. An organic semiconductor is sandwiched between the bottom collector electrode and the top emitter electrode. There is a metallic base with nano-opening in between to control the electric potential profile from the emitter to the base. The operation principle has been reported previously.¹³ The process flow is schematically shown in Fig. 12. Before step (f) it is the same as the nano-channels studied above. Contact coating is used to cover the base in step (g). The organic semiconductor P3HT is deposited in step (h) and the device is finished by evaporating the top Al/MoO₃ emitter electrode. The holes are injected from the emitter into the P3HT valance band, passes through the nano-channel, then reach the collector. Without the base coverage marked in green, the Al base is in contact with P3HT and the holes may either enter the base from the top emitter, or the holes may be injected into the P3HT from the base. Those base currents are to be avoided in the transistor operation. Ideally the base only provides the voltage but no current to turn on and off the emitter-to-collector output current. The process conditions for steps (h)-(i) are given below. After the contact coating step (g) we clean the residue PVPY in the bottom of the channels by 20 seconds, 50W O₂ plasma treatment. Then 1.5 wt% P3HT in chlorobenzene is blade coated.¹⁴ Afterwards, the substrate was annealed at 200° C for 10 minutes. Finally, a 10 nm MoO₃ and a 40 nm Al was deposited on the surface of P3HT in a thermal evaporator.

The SEM images for the complete SCLT with or without base coverage are shown in Fig. 13. P3HT is able to fill in the channel to form the conduction path in both cases. For base coverage to reduce the undesirable leakage current, the most suitable morphology type is the top-only type C defined in Fig. 14(a). The SCLT device structure is shown in Fig. 14(b). We therefore use the condition of 0.004 mm/s pulling speed and 4-5 wt% of PVPY. The details of the covered base is shown in Fig. 1. Note that for this application the PVPY should not fill up or seal the channel, and the bottom collector electrode should not be covered as PVPY is an insulator. It turns out that even for such coating condition there is some PVPY on the channel bottom. That is why before P3HT deposition the channel is cleaned by a second RIE step at 50 W for 20 seconds. Without such RIE

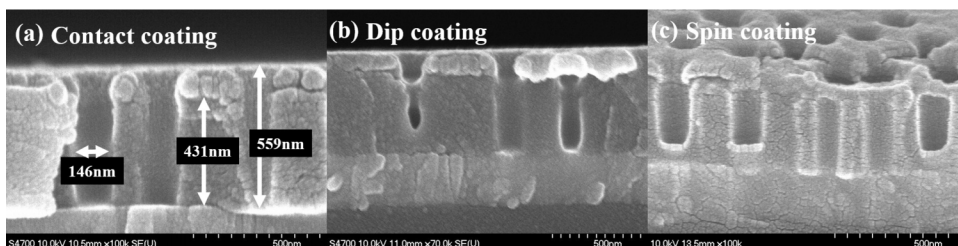


FIG. 11. Other coating methods (a) contact coating, (b) dip coating, and (c) spin coating.

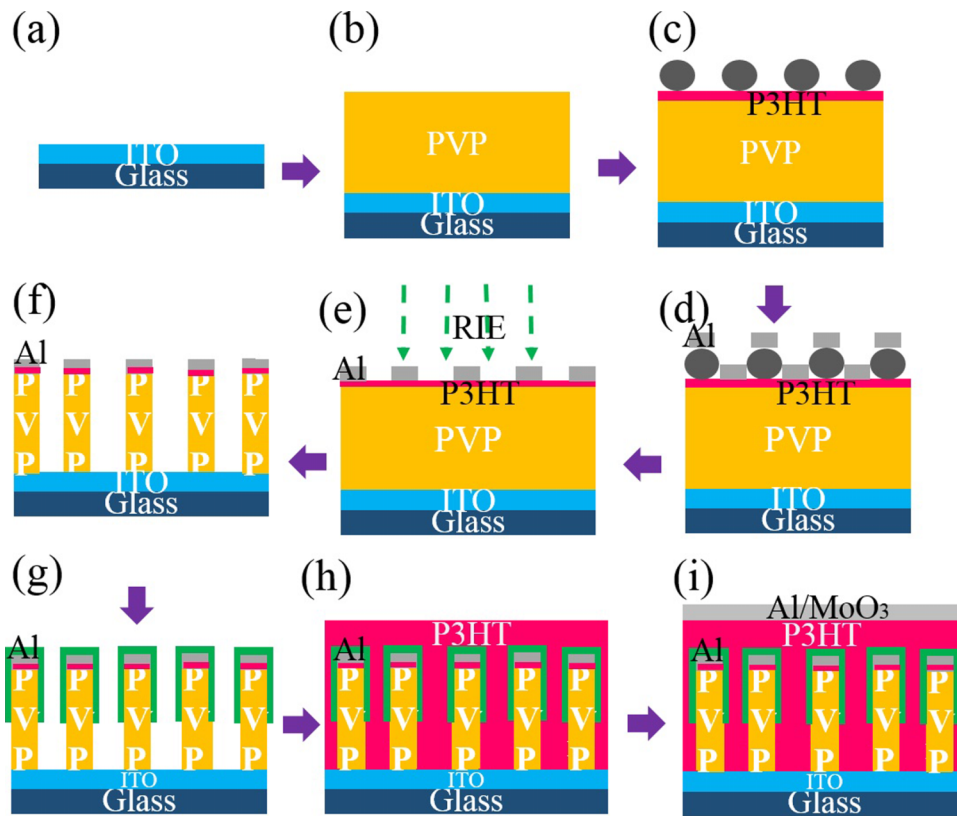


FIG. 12. (a)-(i) The schematic diagram of the nano-channel structure with base coverage fabrication process.

cleaning the transistor output current will be rather low. For PVPY concentration of 4 wt% the characteristics of the transistor with RIE cleaning is shown in Fig. 15 together with the transistor without base coverage. The outstanding effect of base coverage is that the collector voltage endurance is greatly enhanced from about 8V to 15V. With base coverage the base current J_b remains small and stable as V_c increases. Contrarily J_b raises sharply as V_c increases over some threshold without base coverage. The on-off ratio of the transistor is about 5000 at $-V_c=6$ V and 1500 at $-V_c=14$ V. The current gain J_c/J_b is also shown. The second RIE cleaning, however, seems to remove the PVPY on the top surface of the Al base. Because RIE is highly directional, it is likely to spare the PVPY on the channel sidewall and the result is shown schematically in Fig. 16(a). Under high collector voltage bias there is a large voltage drop between base and the collector. Without the base sidewall coverage holes may be injected into P3HT as shown in Fig. 16(b). Such leakage is blocked by the PVPY in the sidewall with base coverage. The top surface of Al base however remain nearly bare so the holes will enter the base once the base is forward biased against the top emitter as shown in

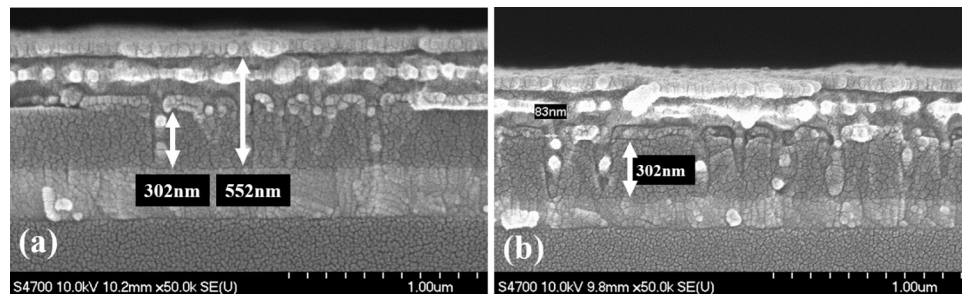


FIG. 13. Cross-section SEM images of the device (a) without base coverage and (b) with base coverage.

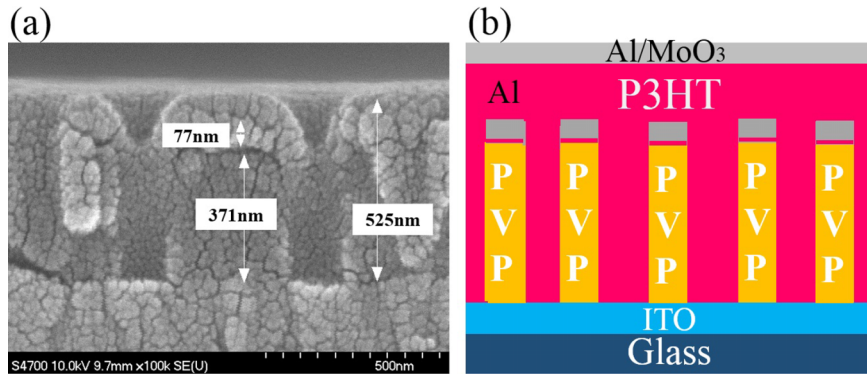


FIG. 14. (a) Cross-section SEM image of the type C 5 wt% and 0.004 mm s^{-1} , and (b) The schematic diagram of device structure.

Fig. 16(c). Indeed the base current J_b raises over 0.01 mA/cm^2 as V_b is too negative, i.e. forward biased at -0.9 V and -1.5 V . To protect the PVPY on top of the Al base we deposit SiO_x of 10 nm at a large tilt angle before the RIE cleaning as shown in Fig. 17(a). Such tilted evaporation covers the top portion of PVPY without insulating the bottom collector electrode. The result for RIE at 50 W for 30 seconds is shown in Fig. 17(b). The base current under forward base bias is now greatly reduced compare with the previous cases in Fig. 18. J_b stays below 10^{-3} mA/cm^2 for V_b and -3.8 V and below 10^{-2} mA/cm^2 for V_b at as high as -4.8 V . This indicates the holes from the top emitter can no longer enter the emitter base even under forward bias as shown in Fig. 17(c). The collector voltage endurance is however not strong as in the previous case without SiO_x tilt evaporation. Somehow the PVPY on the Al base sidewall seems to be removed by the RIE cleaning. The resulting PVPY may be in the form shown in Fig. 17(b), where the top of the Al base is now covered but the sidewall becomes bare. Therefore the hole injection into P3HT is not prevented at

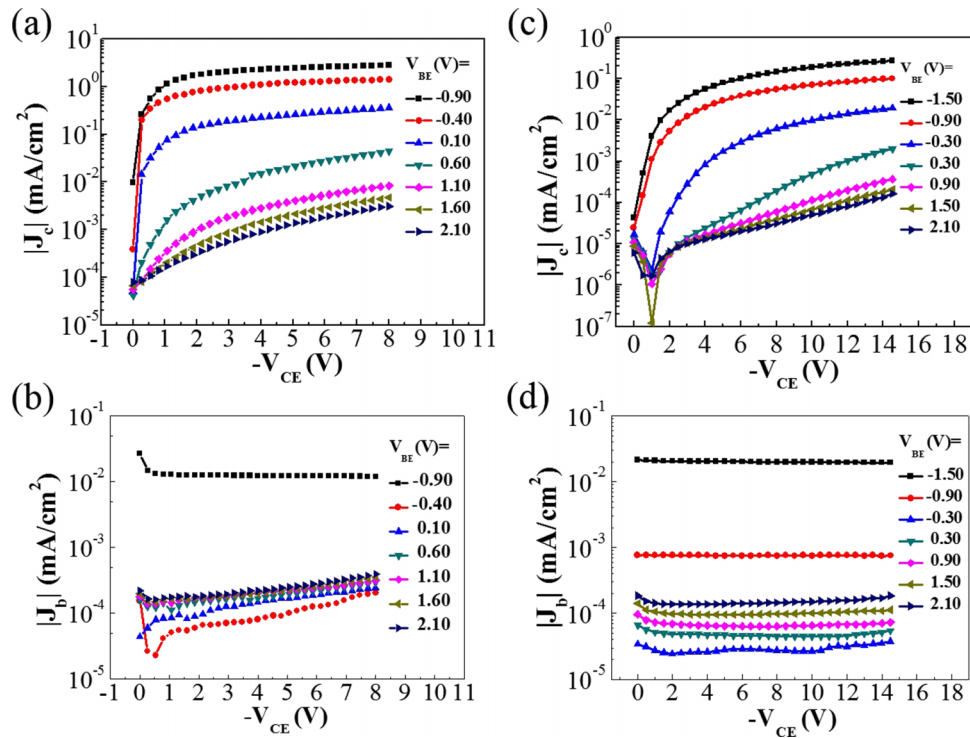


FIG. 15. The output characteristic and base leakage characteristic of the (a)-(b) bare base SCLT and (c)-(d) covered base SCLT.

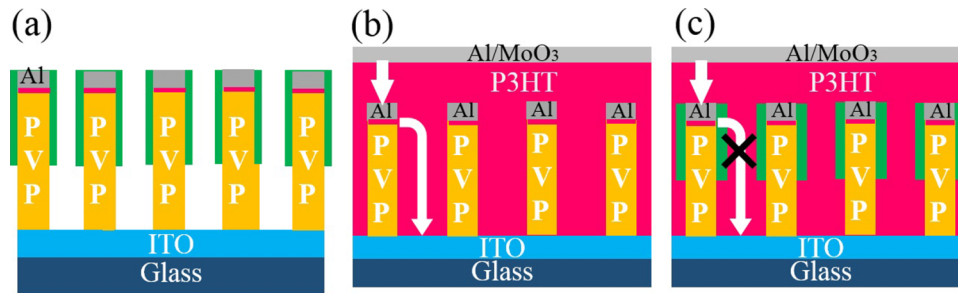


FIG. 16. The schematic diagram of the (a) covered base structure with RIE treatment, (b) leakage path of bare base device, and (c) leakage path of covered base device with RIE treatment.

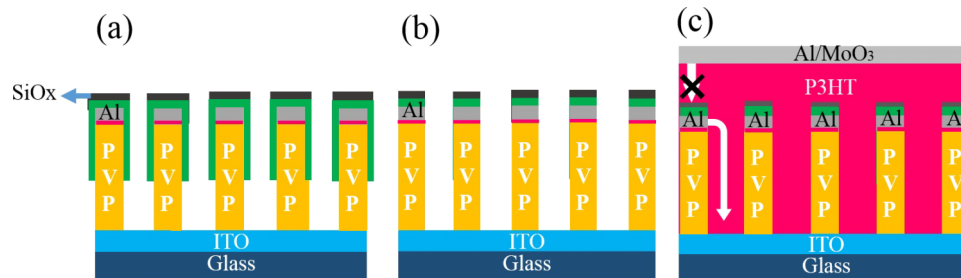


FIG. 17. The schematic diagram of the (a) covered base structure with SiO_x , (b) covered base structure with SiO_x after RIE treatment, and (c) leakage path of covered base device with SiO_x .

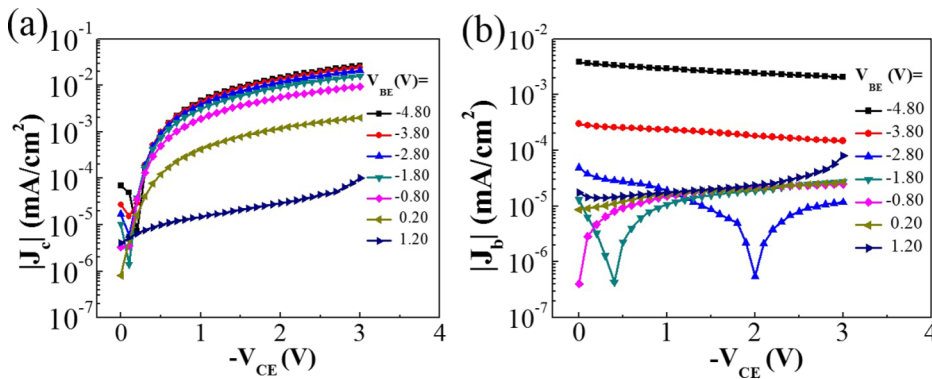


FIG. 18. (a) The output characteristic and (b) base leakage characteristic of the covered base SCLT with SiO_x .

high- V_c . Further works are need to fine tune the coating and RIE condition to realize the optimized device performance. Nevertheless, the increased endurance at higher collector bias and base bias demonstrates the existence of the insulator on the base made by contact coating.

VI. CONCLUSION

A versatile version of contact coating method is developed to cover the nano-structures with various morphologies. In such method the nano-structure surface is kept in contact with the solution surface but not immersed, then pulled up with controlled speed and dried. Due to complex interplay among the surface tension and capillary action during liquid detachment from the surface, the resulting film can be conformal, filled, top-only, or floating depending on the pulling speed and concentration. It is applied in vertical type transistor to cover the base and reduce the leakage current with certain success. Such coating with a wide range of film morphology over nano-structures

in one single platform may find great applications in areas including hybrid solar cell, sensor, and vertical transistors.

ACKNOWLEDGEMENTS

This work was supported by the Ministry of Science and Technology of Taiwan under Contrast No. 102-2120-M-009-008-CC1, No. 101-2112-M-009-006-MY3, and No. 101-2221-E-009-051-MY2.

- ¹ S. R. Tseng, H. F. Meng, K. C. Lee, and S. F. Horng, *Appl. Phys. Lett.* **93**, 153308 (2008).
- ² M. Law, L. E. Greene, J. C. Johnson, R. Saykally, and P. Yang, *Nat. Mater.* **4**, 455 (2005).
- ³ F. Zhang, B. Sun, T. Song, X. Zhu, and S. Lee, *Chem. Mater.* **23**, 2084 (2011).
- ⁴ Y. Cui, Q. Wei, H. Park, and C. M. Lieber, *Science* **293**, 1289 (2001).
- ⁵ M. Uno, Y. Tominari, and J. Takeya, *Appl. Phys. Lett.* **93**, 173301 (2008).
- ⁶ Y. C. Chao, H. F. Meng, and S. F. Horng, *Appl. Phys. Lett.* **88**, 223510 (2006).
- ⁷ P. Yu, C. Y. Tsai, J. K. Chang, C. C. Lai, P. H. Chen, Y. C. Lai, P. T. Tsai, M. C. Li, H. T. Pan, Y. Y. Huang, C. I. Wu, Y. L. Chueh, S. W. Chen, C. H. Du, S. F. Horng, and H. F. Meng, *ACS Nano* **7**, 10780 (2013).
- ⁸ L. He, C. Jiang, Rusli, D. Lai, and H. Wang, *Appl. Phys. Lett.* **99**, 021104 (2011).
- ⁹ C. Y. Chen, K. Y. Wu, Y. C. Chao, H. W. Zan, H. F. Meng, and Y. T. Tao, *Org. Electron.* **12**, 148 (2011).
- ¹⁰ S. C. Shiu, J. J. Chao, S. C. Hung, C. L. Yeh, and C. F. Lin, *Chem. Mater.* **22**, 3108 (2010).
- ¹¹ W. J. D. Silva, I. A. Hümmelgen, and R. M. Q. Mello, *J. Mater. Sci.: Mater. Electron.* **20**, 123 (2009).
- ¹² K. F. Seidel, L. Rossi, R. M. Q. Mello, and I. A. Hümmelgen, *J. Mater. Sci.: Mater. Electron.* **24**, 1052 (2013).
- ¹³ Y. C. Chao and H. F. Meng, *Appl. Phys. Lett.* **88**, 223510 (2006).
- ¹⁴ H. W. Zan, Y. H. Hsu, H. F. Meng, C. H. Huang, Y. T. Tao, and W. W. Tsai, *Appl. Phys. Lett.* **101**, 093307 (2012).